Theoretical study on tertiary amine–fluorophore photoinduced electron transfer (PET) systems

ARTICLE *in* JOURNAL OF MOLECULAR STRUCTURE THEOCHEM · OCTOBER 2008

Impact Factor: 1.37 · DOI: 10.1016/j.theochem.2008.07.025

3 AUTHORS, INCLUDING:

Ioannis D Petsalakis
National Hellenic Research Foundation
142 PUBLICATIONS **1,593** CITATIONS

SEE PROFILE

Nektarios N. Lathiotakis
National Hellenic Research Foundation
62 PUBLICATIONS **1,240** CITATIONS

SEE PROFILE

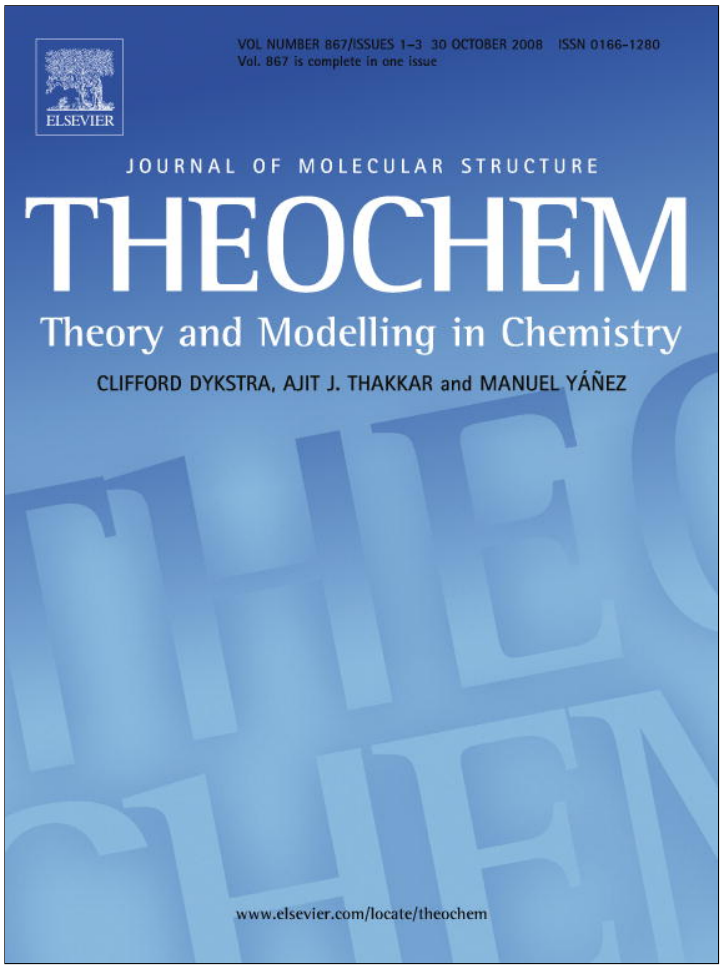

Journal of Molecular Structure: THEOCHEM 867 (2008) 64–70

Contents lists available at ScienceDirect

Journal of Molecular Structure: THEOCHEM

journal homepage: www.elsevier.com/locate/theochem

Theoretical study on tertiary amine-fluorophore photoinduced electron transfer (PET) systems

Ioannis D. Petsalakis, Nektarios N. Lathiotakis, Giannoula Theodorakopoulos *

Theoretical and Physical Chemistry Institute, The National Hellenic Research Foundation, 48 Vassileos Constantinou Avenue, Athens 116 35, Greece

ARTICLE INFO

Article history:
Received 9 June 2008
Accepted 22 July 2008
Available online 31 July 2008

Keywords:
Fluorescent sensors
Photoinduced electron transfer
Density functional theory
Time-dependent density functional theory

ABSTRACT

A series of tertiary amine-fluorophore systems, have been investigated by density functional theory (DFT) and time-dependent density functional theory (TDDFT) calculations. These systems have been proposed as fluorescent sensors for organophosphorus (OP) nerve agent mimics [J. Am. Chem. Soc. 2006, 128, 4500]. The different fluorophores considered are pyrene, coumarin, peryline and coronene. Excitation energies have been determined at the ground state DFT-optimum geometry, with and without the presence of a solvent, yielding information on the absorption spectra of these systems as well as the type of excitation contributing to the relevant excited states. In all these systems, in the initial form, excitations are found characterized by a transfer of electron from the amine to the fluorophore, consistent with the observed quenching of fluorescence. This type of excitations are absent in the corresponding quaternary ammonium systems, resulting from reaction with an OP nerve agent mimic, which is also consistent with the observed fluorescence. A simple rule is proposed for the prediction of the strength of the PET process, based on the degeneracy of the HOMO orbitals calculated for the separate constituent molecules of a sensor system.

1. Introduction

Chemical warfare agents and in particular nerve agents are some of the most dangerous weapons of mass destruction [1]. It is thus of vital interest to develop visual detection methods, based on molecular sensors that indicate the presence of such agents through changes in their fluorescence properties. Recently, a series of systems which might serve as PET sensors for organophosphorus (OP) nerve agent mimics have been proposed and investigated [2]. These systems combine a primary hydroxyl group in close proximity to a tertiary amine, appended with a fluorophore. Fluorescence is generally quenched in the initial system presumably through a photoinduced electron transfer from the amine to the fluorophore. It was found that upon reaction of these compounds with diethyl chlorophosphate (DCP), the corresponding quaternary ammonium salt was produced, with an accompanying increase in fluorescence intensity, by different factors, depending on the particular system [2 and supporting information].

Molecular PET sensors find use in many applications with new systems being reported constantly [3], and it would be of great interest if theoretical information could be obtained on their electronic structure as well as on the photoinduced charge-transfer process. The systems considered here are too large to study with *ab initio* configuration interaction methods, which would be appropriate for calculations on excited electronic states and in particular electron transfer (or charge-transfer) states. However, some useful information on the ground state properties, as well as vertical excitation energies and type of excitation involved can be obtained by DFT [4] and TDDFT [5] calculations, respectively. In a previous publication by the present authors DFT and TDDFT calculations on a PET sensor for dicarboxylic acids were reported, where changes in the intensity of the absorption spectra as well as proton NMR shifts were related to the selective recognition of the different carboxylic acids [6].

In this work, the fluorescent sensor systems of Dale and Rebek [2] mentioned above, have been investigated by DFT and TDDFT calculations, in an effort to obtain information on the electronic structure of these systems and in particular to examine to what extent theoretical information may be used to rationalize the experimental findings and offer predictions regarding the construction of possible PET systems. The calculation of excited states of charge-transfer character is not an easy task, and TDDFT has been often considered as having particular inherent difficulties with such states [7]. However, as already mentioned such methods are realistic alternative methods for systems of this size, at least as a starting point for a theoretical description of photoinduced charge-transfer.

2. Calculations and results

DFT and TDDFT calculations have been carried out on the fluorescent sensor systems presented by Dale and Rebek [2]. In structures **I** below, compounds **1** and **1+** of [2] are indicated as **Ia** and **Ib**,

* Corresponding author. Tel.: +30 210 7273 800; fax: +30 210 7273 794.
E-mail address: ithe@eie.gr (G. Theodorakopoulos).

0166-1280/$ - see front matter © 2008 Elsevier B.V. All rights reserved.
doi:10.1016/j.theochem.2008.07.025

respectively, with one methylene unit linking the amine (or the quaternary ammonium cation) and the fluorophore. In structures **I** small white spheres stand for H atoms, gray spheres for C atoms, blue (dark sphere in grayscale) for N and red for O (dark sphere in grayscale, attached to a C and a H atom, as –C–O–H) atom. In what follows compounds of the type **Ia** (**1** in [2]) will be referred to as initial while those of type **Ib** (**1+** in [2]) as final. For the pyrene-based sensor, in addition to compounds **I**, Compounds **2**, **3**, **4** (and **2+**, **3+**, **4+**) of [2], which have the spacer aliphatic chain increasing to 2, 3 and 4 CH_2 units, respectively, have been calculated. Furthermore, the analogous systems of **Ia** and **Ib** but with different fluorophores than pyrene, namely with coumarin, perylene and coronene have been calculated. All the calculations were performed with the aid of Gaussian 03 [8].

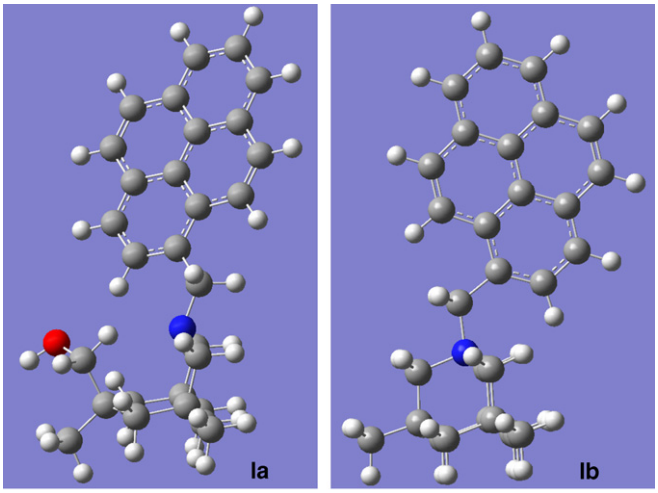

I

Optimum ground state geometries were determined with the aid of DFT calculations, employing the B3LYP functional [9] and the 6-31G (dp) basis set [8]. Subsequently, at the optimum geometry, TDDFT calculations were carried out for each system, involving the 10 lowest singlet excited states. In an effort to better mimic the experimental conditions, the calculations have been performed as well in the presence of a solvent CH_3OH for all systems and CH_2Cl_2 for the coumarin-based sensor only, using the methods of the IEF–PCM model [10 and references therein] provided in Gaussian 03.

An initial study was carried out on the fluorophore molecules alone, see **II** below, with red spheres (dark spheres in grayscale) standing for O atoms in the coumarin molecule. The object of these calculations was to determine the lowest energy intense absorption (i.e. with non-zero calculated oscillator strength), which might be related to the experimental work on the sensor molecules [2]. The results are collected in Table 1, where the wavelength in nm, the associated oscillator strength and the main orbital excitations are given. Experimental data [11,12] and other theoretical [11,13] where available are also included. As these systems attract attention on their own, experimental and theoretical studies on their spectroscopy as well as on substituted forms continue to appear [14]. The present work is focused on the transitions of relevance to the fluorescent sensor systems and the spectroscopy of the fluorophores, in general, is not considered here. As shown in Table 1, in all cases except for coronene in the presence of solvent, the main excitation is a HOMO–LUMO type (i.e. from the highest occupied to the lowest unoccupied orbital), indicated by a superscript in the relevant entries. In general there is good agreement with experimental data and other theoretical work on the fluorophore molecules alone. The effect of the solvent varies for the different

Table 1
Results of the TDDFT calculations on the lowest singlet excitations with non-zero oscillator strength of the fluorophore molecules without and with the presence of solvent

(i)	Pyrene	Pyrene + solv.	Coumarin	Coumarin + solv.
λ (nm), f-val	340, 0.28 336[b], 0.27[b]	338, 0.36 333[c], 367[d], 0.21[d]	329, 0.26	339, 0.33
Excitation	53→54[a] 52→55	53→54[a] 52→55	54→55[a] 53→55 53→56	54→55[a] 53→55 53→56
(ii)	Perylene	Perylene + solv.	Coronene	Coronene + solv.
λ (nm), f-val	428, 0.36	439, 0.45 437[e], 0.81[e]	299, 0.66	305, 0.89 305[f], 4.9[f]
Excitation	66→67[a] 62→69	66→67[a]	78→79[a] 77→80 78→80 77→79 76→83 75→81	78→80 77→79 74→81

[a] HOMO-LUMO excitation.
[b] Other theoret [13].
[c] Exper [11].
[d] Other theoret [11].
[e] Exper (S_p) [12].
[f] Exper. [12].

systems and excited state, and it is for most cases a small shift towards the blue or the red, leaving the character of the calculated state unaffected.

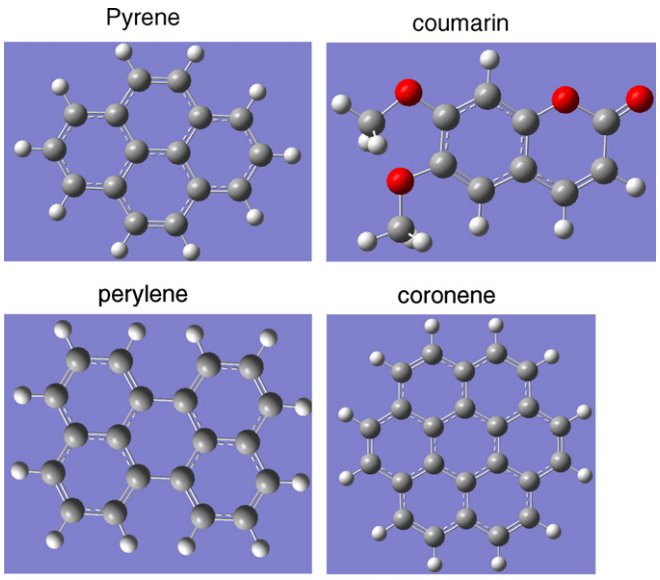

II

Next the initial and final structures, **Ia** and **Ib** of the pyrene-based sensor molecule as well as the coumarin-based, perylene-based and coronene-based analogues have been calculated, both as isolated molecules and in methanol (in CH_2Cl_2 for coumarin-based sensor) solvent. The object of the calculations in the sensor molecules was to relate, if possible, their results to the observed suppression of fluorescence in the initial structures and the lifting of the suppression in the final structures, (cf. **Ib** in **I**), which are cations. As the suppression of fluorescence in the initial systems has been attributed to a transfer of electrons from the amine group to the fluorophore, it is of interest to determine the excitations in the region of interest in each case, in an effort to identify possible charge-transfer type of excitations, which would be instrumental in the photoinduced suppression of fluorescence. The results of

the TDDFT calculations are collected in Tables 2–5, for the pyrene-, coumarin-, perylene- and coronene-based systems, respectively, where in these Tables, the superscript a denotes charge-transfer type excitation. The following may be noted from results on the pyrene-based sensor molecule, see Table 2: Calculations on the isolated **Ia** system obtain the third lowest transition as the one involving transfer of an electron from the amine to the pyrene group (excitation 110→112 in Table 2, second column). Upon introduction of the solvent (methanol), the charge-transfer type excitation is found to contribute to all three lowest energy transitions (listed under "initial + solv", third column of Table 2). This is shown pictorially in Fig. 1, where the orbitals involved in the main excitations contributing to the lowest energy absorption in the pyrene-based sensor in methanol have been plotted. As shown, while the HOMO and HOMO-2 orbitals (as also LUMO and LUMO+1) are located on pyrene, HOMO-1 is located on the amine section of the molecule. The existence of this charge-transfer contribution (HOMO-1 → LUMO) to the excited states of the initial system is consistent with a nonadiabatic interaction of the absorbing state with a charge-transfer state which will cause a suppression of the fluorescence. Conversely, such excitation is not found in the excited states of the final cationic form of the pyrene-based sensor system, where all of the higher-lying occupied orbitals (the six highest) are located on the fluorophore. And it should be mentioned here, to save repetition, that this is the case for all the final forms of the sensor molecules calculated in the present work. A similar situation as the initial form of pyrene-based sensor molecule is found in the results of the calculations on the coumarin-based molecule, as shown in Table 3. In this case, it is the second transition calculated that is relevant to the experimental absorption spectrum, as shown by a comparison with the experimental absorption maximum at 347 nm [2]. Furthermore, the first transition has 0.0 oscillator strength. However, this lowest transition of the initial system in solvent corresponds to the charge-transfer type of excitation, again consistent with non-radiative interaction of the absorbing state with the lower-lying charge-transfer state and suppression of emission in the initial system. In Fig. 2, the orbitals relevant to the lowest two transitions calculated for the initial form of the coumarin-based sensor are shown. As in the pyrene-based system, the presence of the solvent resulted in having the charge-transfer excitation contributing to a lower state than in the isolated molecule (see Table 3). For the case of the perylene-based sensor molecule, the charge-transfer excitation characterizes the second singlet excited state of the initial system, again with zero oscillator strength,

Table 2
Results of TDDFT calculations on the pyrene-based sensor molecules

	Initial (**Ia**)	Initial + solv.	Final (**Ib**)	Final + solvent
λ_1 (nm), *f*-val	343, 0.35	349, 341[b], 0.40	350, 0.33	350, 344[b], 0.46
Excitation	109→113	109→113	105→108	105→108
	111→112	110→112[a]	106→107	106→107
		111→112		
λ_2 (nm), *f*-val	332, 0.0	338, 0.07	335, 0.01	332, (330) 0.0
Excitation	109→112	109→112	105→107	105→107
	111→113	110→112[a]	106→108	106→108
		111→112		
		111→113		
λ_3 (nm), *f*-val	320, 0.1	331, 0.01	287, 0.07	281, 0.04
Excitation	110→112[a]	109→112	104→107	104→107
		110→112[a]	105→107	105→107
		111→113	106→108	106→108
			106→109	106→109

[a] Charge-transfer excitation.
[b] Experimental [2].

Table 3
Results of TDDFT calculations on the coumarin-based sensor molecule

	Initial	Initial + solv.	Final	Final + solvent
λ_1 (nm), *f*-val	370, 0.0	398, 0.0	387, 0.18	372, 379[b], 0.24
Excitation	111→113	112→113[a]	106→108	106→108, 106→109
			106→109	107→108
			107→108	
λ_2 (nm), *f*-val	338, 0.19	345,347[b], 0.25	302, 0.01	299, 0.14
Excitation	110→113	110→113	105→108,	106→108
	110→114	110→114	106→108,	107→109
	112→113[a]	111→113		
λ_3 (nm), *f*-val	281, 0.0	284, 0.13	302, 0.11	249 (fourth root)[c], 0.0
Excitation	108→113	110→113	105→108,	105→108,
	108→115	111→114	106→108,	106→109
	109→113[a]		107→109	107→109, 107→110

[a] Charge-transfer excitation.
[b] Experimental [2].
[c] The third root at λ = 271 nm is characterized by 104→108 and 104→110.

Table 4
Results of TDDFT calculations on the lowest three transitions in the perylene-based sensor molecule

	Initial	Initial + solv.	Final	Final + solvent
λ_1 (nm), *f*-val	435, 0.44	445, 439[b], 0.53	446, 0.45	446, 443[b], 0.55
Excitation	124→125	124→125	119→120	119→120
λ_2 (nm), *f*-val	349, 0.0	376, 0.0	343, 0.01	336, 0.0
Excitation	123→125[a]	123→125[a]	115→120	117→120
			117→120	118→120
			118→120	119→121
			119→121	
			119→125	
λ_3 (nm), *f*-val	335, 0.0	336, 0.0	329, 0.0	314, 0.0
Excitation	122→125	122→125	116→120	116→120
	124→126	124→126	117→120	117→120
	124→127	124→127	118→120	118→120
			119→121	119→121
			119→122	119→122
			119→125	119→124

[a] Charge-transfer excitation.
[b] Experimental [2].

Table 5
Results of TDDFT calculations on the coronene-based sensor molecules

	Initial	Initial +solv.	Final	Final +solvent
λ (nm), *f*-val	387, 0.0	386, 0.0	393, 0.01	387, 0.0
Excitation	135→137	135→137	130→132	130→132
	135→138	135→138	130→133	130→133
	136→137	136→137	131→132	131→132
	136→138	136→138	131→133	131→133
λ (nm), *f*-val	305 (third root), 0.25	309 (fifth)[c], 307[b], 1.0	316 (third), 0.38	310 (third), 309[b], 0.82
Excitation	134→137[a]	134→138[a]	130→132	130→132
	134→138[a]	135→137	130→133	130→133
	135→137	135→138	130→134	131→132
	135→138	136→137	131→132	131→133
	136→137	136→138	131→133	
	136→138		131→134	
λ (nm), *f*-val	303 (fourth), 0.64	308 (sixth), 0.80	311 (fourth), 0.72	310 (fourth), 0.99
Excitation	134→137[a]	134→137[a]	130→132	130→132
	134→138[a]	135→137	130→133	130→133
	135→137	135→138	131→132	131→132
	135→138	136→137	131→133	131→133
	136→137	136→138	131→134	
	136→138			

[a] Charge-transfer excitation.
[b] Experimental [2].
[c] The third and fourth root calculated at 328 and 323 nm, respectively, involve mainly the 134→137 and 134→138 excitations.

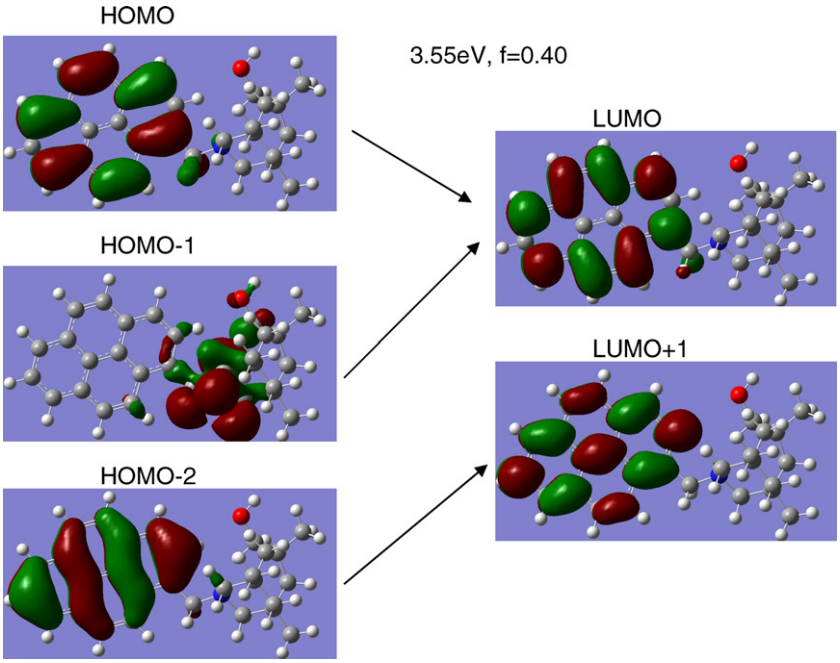

Fig. 1. Electron density plots of the frontier orbitals in the initial form of the pyrene-based sensor. HOMO-1 → LUMO is the charge-transfer excitation.

while the absorbing state is the lowest excited state. In this case it might be envisaged that at some other geometry than that of the ground state, the two excited states (the absorbing state and the charge-transfer state) may come close together leading to transfer of population to the charge-transfer state and suppression of emission in the initial form. The orbitals relevant to the excitations mainly contributing to the two excited states of the perylene-based sensor system have been plotted in Fig. 3, whereas the results on the coronene-based sensor are summarized in Table 5 and the relevant orbital electron density plots are given in Fig. 4. As shown in Table 5, the transition relevant to the experimental observations of the coronene-based sensor [2] is not the lowest excited state calculated but a higher root, which in the isolated initial system is the third root but in the presence of solvent it is the fifth root calculated. For the final cationic systems, it is the third root both in the isolated system and in the presence of solvent (see Table 5). In this molecule degeneracy/near degeneracy between different excited states is found, as for example between the third

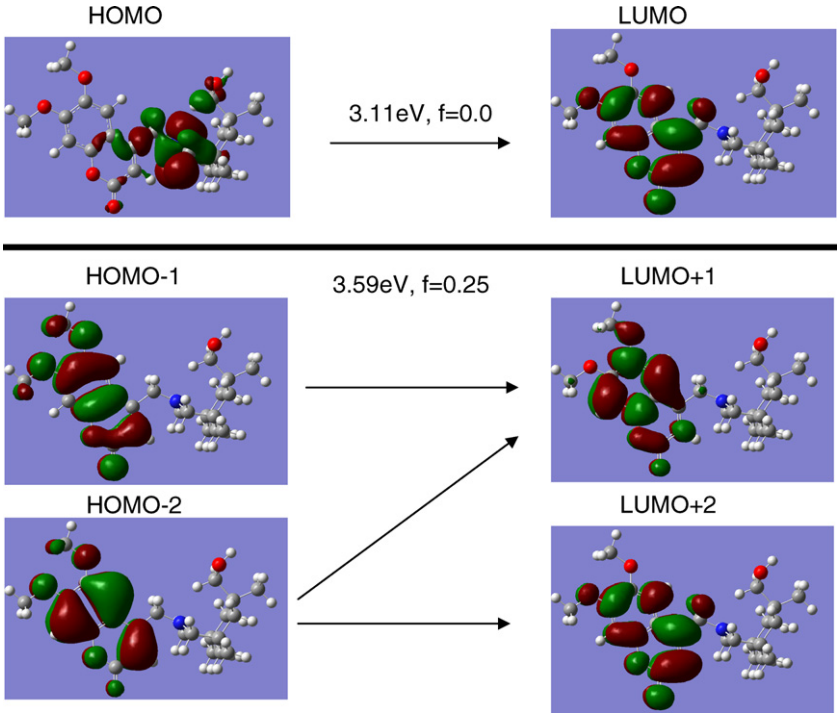

Fig. 2. Electron density plots of the frontier orbitals in the initial form of the coumarin-based sensor. Upper section relevant to the first excited state, lower part relevant to the second excited state. HOMO → LUMO is the charge-transfer excitation.

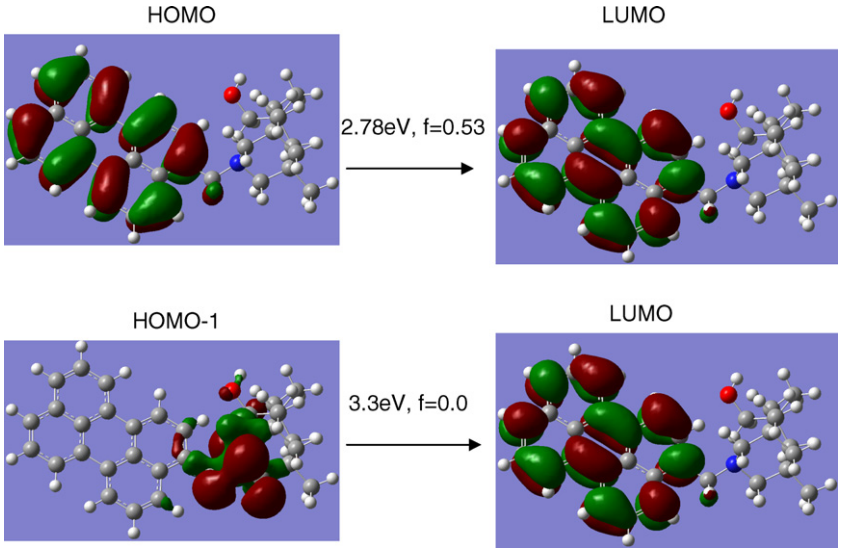

Fig. 3. Electron density plots of the frontier orbitals in the initial form of the perylene-based sensor. Upper section relevant to the first excited state, lower part relevant to the second excited state. HOMO-1 → LUMO is the charge-transfer excitation.

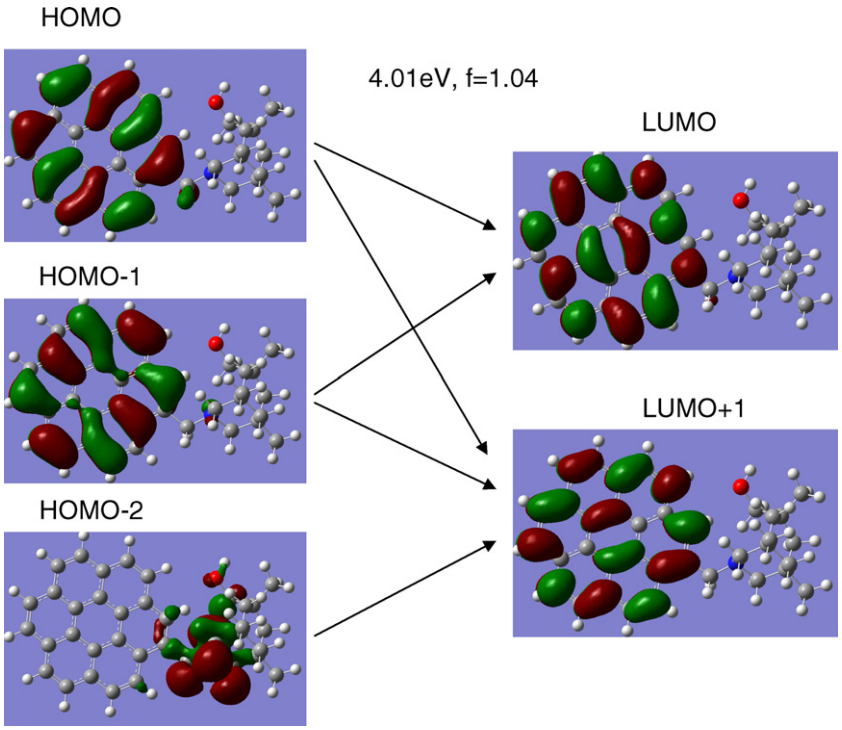

Fig. 4. Electron density plots of the frontier orbitals in the initial form of the coronene-based sensor. HOMO-2 → LUMO+1 is the charge-transfer excitation.

and fourth (fifth and sixth initial + solvent) states, in Table 5, with the charge-transfer excitation contributing to both these states in the initial sensor molecule. Furthermore, for the initial sensor molecule in the presence of solvent the third and fourth excited states involve mainly charge-transfer excitations, with oscillator strength 0.01 and 0.03, respectively. These states are not calculated as such in the absence of solvent, but are found as the fifth and sixth states (not included in Table 5), to which a number of excitations contribute, including the charge-transfer ones. Thus the effect of the solvent is to stabilize or lower the energy of the charge-transfer excitations. This was also found in the cases of pyrene-based and coumarin-based sensor molecules, but not in the same manner as in the coronene-based sensor. For the final form of all the sensor systems (analogous to **Ib** in **I**), the effect of the solvent is not striking, involving mainly shifts towards higher energies and leaving the states for the most part unaffected.

It is possible to draw conclusions on the photoinduced charge-transfer in these systems and possibly generalize them for other systems, if the two parts of molecules **Ia** are considered separately, for example pyrene and the tertiary amine with a $-CH_3$ group instead of $-CH_2$-pyrene at N and similarly for **Ib**. The orbital energies of the frontier orbitals in these systems are plotted in Fig. 5, where it is shown that the HOMO energies of separate pyrene and tertiary amine-alcohol are nearly degenerate. In the sensor system, the degeneracy is lifted but still the two levels are close in energy, with the result that the PET transition is very close in energy to the

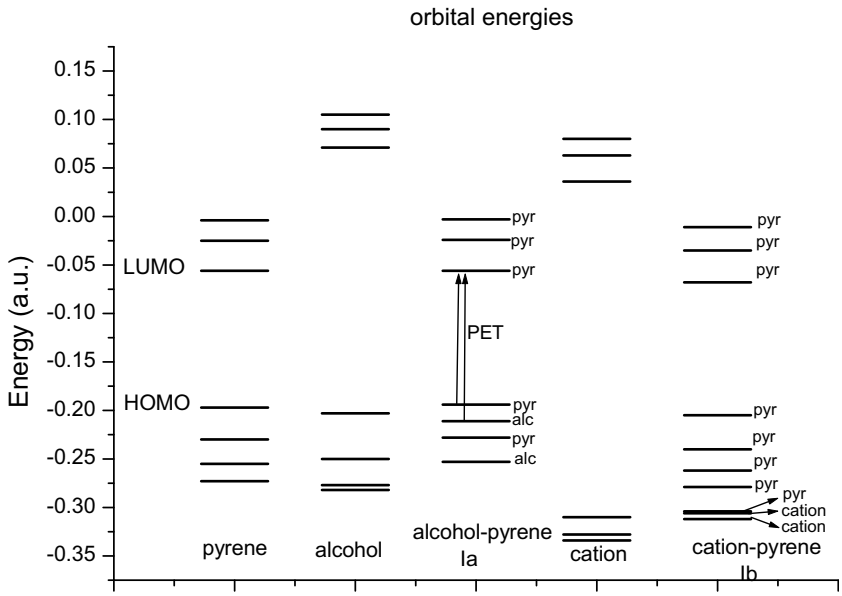

Fig. 5. Orbital energy levels of pyrene, t-amine-alcohol, pyrene-based sensor initial (**Ia**), cyclic quaternary ammonium fragment and final form of the sensor (**Ib**).

absorption in pyrene. In the final system (quaternary ammonium cation), the orbital energies of the two fragments are well separated, and all the lower energy transitions involve the pyrene spectrum. The near degeneracy of the HOMO orbital energies of the separate fragments is thus one of the requirements for a PET system while the degree of degeneracy might be a measure of the strength of the PET process. In Table 6, the orbital energies of the different fluorophores are given along with those of the t-amine-alcohol. For pyrene and coumarin the HOMO energies are −0.197 and −0.208 hartree, compared to −0.203 of the t-amine-alcohol fragment (cf. Table 6). Accordingly, a strong suppression of fluorescence is found in the corresponding (**Ia**) sensor systems, as indicated by the 22-fold and 20-fold increase in fluorescence of the final system, respectively [2]. The HOMO energy of perylene is calculated as −0.184 hartree, not as close to −0.203 as the previous two systems and accordingly only about a 3-fold increase in fluorescence is obtained in the final (**Ib**) versus the initial (**Ia**) form of the perylene-based sensor [2]. Thus for these three sensors the simple HOMO degeneracy argument is consistent with the observed results. In the case of the coronene-based system, the situation is more complicated by the existence of degeneracy in the two highest occupied orbitals of coronene, at −0.201 hartree, very close to −0.203 of the amine fragment (see Table 6). However, the experimental observation for the coronene-based sensor is that there is only a 2-fold increase in fluorescence in the final form. This might be rationalized by the theoretical result that the two highest occupied orbitals of the combined coronene-based system (ninth column of Table 6) belong to coronene (cf. Fig. 4), and only HOMO-2 belongs to amine, thus diminishing the significance of the charge-transfer excitation.

The above results on the different sensor molecules are consistent with the suppression of emission in the initial sensor molecules and the lifting of the suppression in the final cationic form, which makes these systems useful as sensors for organophosphorus nerve agent mimics, according to the experimental work [2].

On the basis of the present calculations, it is not possible to rationalize the trend found experimentally in the series from 1 to 4, where spacers of different length are involved between the amine and the fluorophore molecules. Relevant calculations have been carried out for the pyrene-based sensor, in an effort to reproduce the trend of decreasing suppression of emission with increasing number of methylene units in the spacer [2]. As shown in Fig. 6, the HOMO and LUMO orbitals remain basically the same, independent of the size of the spacer. Similarly, the results of the TDDFT calculations are similar for systems 1–3 (i.e. from 1 to 3 CH_2 units in the spacer), with the charge-transfer excitation contributing to the lowest excited state, in the presence of solvent, with λ of 348–351 nm and *f*-value of 0.40–0.46. For system 4, the charge-transfer excitation characterizes the second excited state, with λ of 331 nm and *f*-value 0.0018. So in this sense, compound 4 is different from compounds 1–3. However, this is not enough to rationalize the lack of suppression of emission in 4, since in the perylene-based sensor molecule where a similar type of contribution of the charge-transfer excitation to the state above the absorbing state is found, there is a suppression of emission [2]. Therefore, one would need to examine in detail the geometry of the excited

Table 6
Orbital energies (3 unoccupied, 4 occupied) of the different sensor systems (**Ia** form) and fragments

Alcohol	Pyre.	Pyre. **Ia**	Coum.	Coum. **Ia**	Pery.	Pery. **Ia**	Coro.	Coro. **Ia**
0.105	−0.004	−0.003	0.007	0.007	−0.008	−0.006	−0.012	−0.013
0.090	−0.025	−0.024	0.000	−0.009	−0.018	−0.018	−0.054	−0.052
0.071	−0.056	−0.056	−0.061	−0.060	−0.071	−0.071	−0.054	−0.054
−0.203	−0.197	−0.194	−0.208	−0.202	−0.184	−0.182	−0.201	−0.200
−0.250	−0.230	−0.211	−0.240	−0.218	−0.243	−0.211	−0.201	−0.201
−0.277	−0.255	−0.228	−0.278	−0.248	−0.249	−0.242	−0.251	−0.212
−0.282	−0.273	−0.253	−0.283	−0.253	−0.252	−0.247	−0.251	−0.247

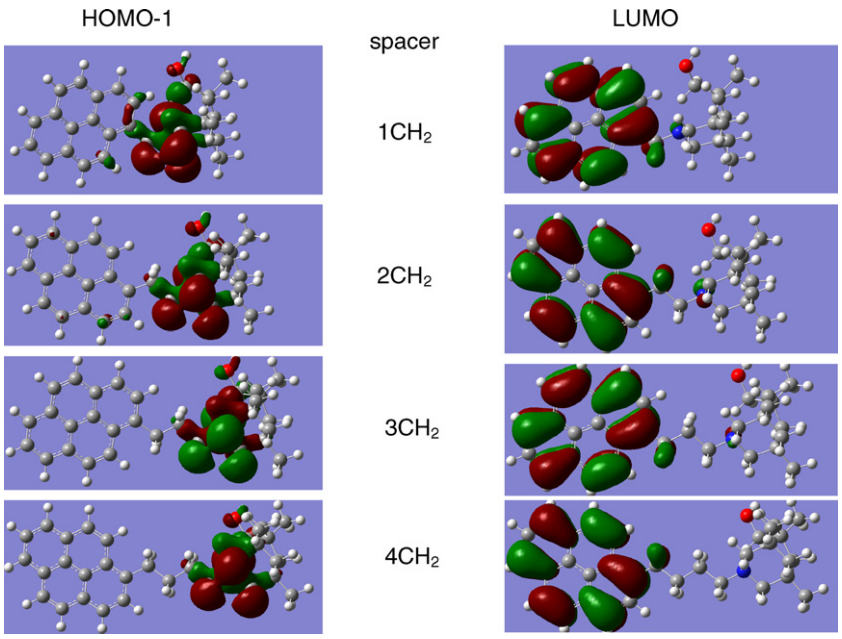

Fig. 6. Electron-density plots of the HOMO-1 and LUMO orbitals in the pyrene-based sensor, involving different spacer, from 1 to 4 CH_2 units between the amine and pyrene.

states, and if possible to calculate the nonadiabatic interactions in order to obtain information which might be consistent with the experimental findings along the series of compounds 1–4 [2].

3. Conclusion

Fluorescent sensor molecules are of great importance and in particular those that may serve for sensing the existence of warfare agents. In the present work DFT and TDDFT calculations have been carried out on a series of fluorescent sensors for organophosphorus nerve agent mimics. The present calculations are relevant to the vertical energy spectrum, at the optimum geometry calculated for the ground electronic state, and the object is to obtain theoretical information consistent with the suppression of fluorescence in the initial form of the sensor molecules and the lifting of this suppression in the final form, which results following the reaction with the nerve agent mimic compound. The present results show that for the different sensors examined, pyrene-, coumarin-, perylene- and coronene-based sensor systems, with a single CH_2 group as spacer between the amine and the fluorophores, charge-transfer excitations (from the amine to the fluorophore) are identified contributing either to the character of the absorbing state or to a lower-lying state, or a close-lying higher electronic state. This contribution is interpreted as evidence for non-radiative interaction of the absorbing state with a charge-transfer state, and subsequent transfer of population, leading to a suppression of emission. Such contribution does not exist in the final cationic form, and emission of the fluorophore is not suppressed. The effect of solvation was also studied and it was found to lower the energy of the state to which charge-transfer excitation contributes. Calculations on pyrene-based sensors involving spacers consisting of 2, 3 and 4 CH_2 units do not yield information consistent with the experimental observation of diminishing suppression of fluorescence in the above series [2]. Finally, on the basis of the orbital energies, a simple general rule is recognized, namely that a PET process between two different sections of a sensor system will be stronger when there is near degeneracy of the HOMO of the different sections, at least in the simpler cases where there are no degeneracies in the highest occupied orbitals of the fluorophore.

Acknowledgements

Partial financial support from the EU FP7, Capacities Program, NANOHOST project (GA 201729) is acknowledged. Partial support of this work through the "Excellence in the Research Institutes" program, supervised by the General Secretariat for Research and Technology/Ministry of Development, Greece (Phase I and II, Projects 64769 and 2005ΣΕ01330081), is gratefully acknowledged. The authors are grateful to Dr. N. Tagmatarchis for helpful discussions. The authors are grateful to Prof. J. Rebek Jr. and Dr. T.J. Dale for helpful communication.

References

[1] M. Burnworth, S.J. Rowan, C. Weder, Chem. Eur. J. 13 (2007) 7828.
[2] T.J. Dale, J. Rebek Jr., J. Am. Chem. Soc. 128 (2006) 4500.
[3] J.-J. Lee, B.C. Noll, B.D. Smith, Org. Lett. 10 (2008) 1735.
[4] R.G. Parr, W. Yang, Annu. Rev. Phys. Chem. 46 (1995) 701.
[5] M.A.L. Marques, E.K.U. Gross, Annu. Rev. Phys. Chem. 55 (2004) 427.
[6] I.D. Petsalakis, N. Tagmatarchis, G. Rotas, G. Theodorakopoulos, J. Mol. Struct. (THEOCHEM) 807 (2007) 11.
[7] A. Dreuw, M. Head-Gordon, Chem. Rev. 105 (2005) 4009.
[8] M.J. Frisch, G.W. Trucks, H.B. Schlegel, G.E. Scuseria, M.A. Robb, J.R. Cheeseman, J.A. Montgomery Jr., T. Vreven, K.N. Kudin, J.C. Burant, J.M. Millam, S.S. Iyengar, J. Tomasi, V. Barone, B. Mennucci, M. Cossi, G. Scalmani, N. Rega, G.A. Petersson, H. Nakatsuji, M. Hada, M. Ehara, K. Toyota, R. Fukuda, J. Hasegawa, M. Ishida, T. Nakajima, Y. Honda, O. Kitao, H. Nakai, M. Klene, X. Li, J.E. Knox, H.P. Hratchian, J.B. Cross, C. Adamo, J. Jaramillo, R. Gomperts, R.E. Stratmann, O. Yazyev, A.J. Austin, R. Cammi, C. Pomelli, J.W. Ochterski, P.Y. Ayala, K. Morokuma, G.A. Voth, P. Salvador, J.J. Dannenberg, V.G. Zakrzewski, S. Dapprich, A.D. Daniels, M.C. Strain, O. Farkas, D.K. Malick, A.D. Rabuck, K. Raghavachari, J.B. Foresman, J.V. Ortiz, Q. Cui, A.G. Baboul, S. Clifford, J. Cioslowski, B.B. Stefanov, G. Liu, A. Liashenko, P. Piskorz, I. Komaromi, R.L. Martin, D.J. Fox, T. Keith, M.A. Al-Laham, C.Y. Peng, A. Nanayakkara, M. Challacombe, P.M.W. Gill, B. Johnson, W. Chen, M.W. Wong, C. Gonzalez, J.A. Pople, Gaussian 03, Revision C.02, Gaussian, Inc., Wallingford CT, 2004.
[9] A.D. Becke, J. Chem. Phys. 98 (1993) 5648;
C. Lee, W. Yang, R.G. Parr, Phys. Rev. B. 37 (1989) 785.
[10] M. Cozi, G. Scalmani, N. Rega, V. Barone, J. Chem. Phys. 117 (2002) 43.
[11] J. Neugebauer, E.J. Baerends, E.V. Efremov, F. Ariese, C. Gooijer, J. Phys. Chem. A 109 (2005) 2100.
[12] N. Nijegorodov, R. Mabbs, W.S. Downey, Spectrochim. Acta A 57 (2001) 2673.
[13] M. Dierksen, S. Grimme, J. Chem. Phys. 120 (2004) 3544.
[14] O. Birer, P. Moreschini, K.K. Lehmann, Phys. Chem. Chem. Phys. 10 (2008) 1648;
R. Improta, V. Barone, F. Santoro, J. Phys. Chem. B 111 (2007) 1480.